Perfectly Matched Layer Finite Element Simulation of Parasitic Acoustic Wave Radiation in Microacoustic Devices

Markus Mayer*, Sabine Zaglmayr†, Karl Wagner* and Joachim Schöberl‡
* EPCOS AG, Surface Acoustic Wave Components, Munich, Germany
† FWF-Startprojekt Y-192, J. Radon Institute for Computational and Applied Mathematics, Linz, Austria
‡ Department of Mathematics CCES, RWTH Aachen University, Aachen, Germany

***Abstract*—Classical finite element methods are only capable of describing a limited computation area; the substrate of a microacoustic device must therefore be described by suitable boundary conditions. This is obtained by absorbing boundary conditions (ABC) or perfectly matched layers (PML) which both suppress reflections from the substrate. PML was implemented into a high-performance finite element code. The employed variant of the PML approach relies on a complex variable transformation of the basic piezoelectric equations in the PML layer. Harmonic admittances of a system with aluminum electrodes on a 42° YX-$LiTaO_3$ substrate are determined with PML and ABC methods and compared to FEM/BEM results, which can be considered as exact solution of the piezoelectric half space problem. The results of PML approach FEM/BEM, while the ABC results deviate. The correct adjustment of PML parameters to minimize reflection at the substrate/PML interface is illustrated by visualizations of the wave fields.**

I. Introduction

Ab initio simulations, i.e. simulations solving the basic piezoelectric equations, are of increasing importance in the design of microacoustic devices. To date ab initio simulations of complete devices are still too slow to be employed in the optimization stage of device design. The state of the art technique is to consider a unit cell with periodic boundary conditions and to compute the harmonic admittance [1]. Therefrom parameters for computationally fast P-matrix or COM simulations are derived [2], [3].

The method of choice for harmonic admittance computations is the finite element method (FEM), allowing for a high flexibility in the definition of device structures. As long as the electro acoustic wave is spatially confined FEM is sufficient. In many applications as in the case of leaky surface acoustic waves (LSAW) considered in this work, energy is radiated to the substrate. This problem can be dealt with by introducing suitable non-reflecting boundary conditions at the bottom (without lack of generality the substrate is considered to occupy the lower half space) of the computation area in order to mimic an infinitely extended substrate. A rigorous approach to do so is to employ the boundary element method (BEM) [4], [5], which provides an exact solution of the problem. The disadvantage of this FEM/BEM approach is on one hand that it is non-local, since it couples all degrees of freedom at the boundary and thus destroys the sparsity of the FEM system of equations. On the other hand the implementation is in general more involved since a Green's function needs to be computed.

Higher flexibility is provided by absorbing boundary conditions (ABC) or perfectly matched layers (PML). Absorbing boundary conditions state a local approximation of perfectly absorbing BCs, e.g. by n-th order differential operators [6] or by compositions of first-order differential operators [7]. These transparent BC have local character, but are reflectionless only for a discrete set of space directions.

A more convenient approach is provided by PML. The idea is to introduce an absorbing layer where propagating as well as evanescent waves are transformed to highly attenuated waves. The method was introduced by Berenger [8] for electromagnetic problems and can be interpreted as a complex transformation of space coordinates [9], [10]. The PML-parameters are chosen to guarantee a sufficiently fast attenuation within the layer such that the reflections - caused by imposing Dirichlet or Neumann BCs at the outer PML-boundary - are negligibly small. On the continuum level, the absorbing layer is reflectionless for all angles of incidence and all frequencies. Nevertheless, spurious reflections can be introduced by discretization at the artifical interface boundary.

Periodic FEM with ABC has been implemented recently into the Netgen/NGsolve package [11]. Within the present work the PML method for piezoelectric equations was added.

The paper is organized as follows: In section II the theoretical background of the incorporation of PML for piezoelectric equations and its combination with the quasi-periodic FEM is presented. In chapter III the first-order ABC, PML and BEM methods to describe the infinite substrate are compared at the example of the bulk wave radiation description for the leaky wave substrate 42° YX-$LiTaO_3$.

II. Theory

A. The governing piezoelectric equations

We view the linear piezoelectric equations in a time-harmonic setting for the mechanical displacement $\mathbf{u}$ and the electric potential Φ which read as

$$-div\,\mathbb{T} - \omega^2\rho\mathbf{u} = \mathbf{f} \tag{1}$$

$$-div\,\mathbf{D} = \mathbf{q} \tag{2}$$

with linear material laws

$$\mathbb{T}_{ij} = c_{ijkl}\,\mathbb{S}_{kl} - e_{kij}\,\mathbf{E}_k, \tag{3}$$

$$\mathbf{D}_i = e_{ikl}\,\mathbb{S}_{kl} + \varepsilon_{ik}\,\mathbf{E}_k, \tag{4}$$

and

$$\begin{array}{ll} \text{elastic strains} & \mathbb{S} = \frac{1}{2}(\nabla\mathbf{u} + (\nabla\mathbf{u})^t) \\ \text{and the electric field} & \mathbf{E} = -\nabla\Phi, \end{array}$$

where $\mathbf{f}$ and $\mathbf{q}$ are mechanical and electrical sources, respectively and $\omega = 2\pi f$, with frequency f. Above material parameters denote the mechanical stiffness tensor c at constant electric field, the piezoelectric coupling tensor e at constant strain, the dielectric permittivity tensor ε at constant strain, and the density ρ (see [12]).

B. The idea and design of PML for piezoelectric equations

The method of perfectly matched layers became recently a popular concept of truncating spatially unbounded domains the way that only outgoing waves are realized and reflections at the introduced artificial boundary are suppressed. On the continuum level it realizes a reflectionless ABC for all angles of incidence and all frequencies (cf. [8], [9]).

The idea bases on the construction of an outer boundary layer Ω_{PML} such that

- the solution/equations remains unchanged in the domain of interest Ω_O,
- propagating waves are converted to evanescent ones in the PML Ω_{PML},
- the exponential decay of the waves in the PML is sufficiently strong in order to justify the truncation of the outer PML boundary by homogeneous boundary conditions, i.e. reflections at the outer boundary are negligibly small.

In view of the discrete level we assume a sufficiently good discretization around the artificial interface $\Omega_O \cap \Omega_{PML}$ in order to suppress spurious reflections.

The principle of perfectly matched layers relies on an analytic continuation of the underlying equations/solution into the complex plane. This can be realized by a *complex coordinate-stretching* [9] as done for the cartesian-coordinates x_i, i=1,2 by introducing

$$x_i \to z_i(x_i) := x_i + a_i(x_i) - ib_i(x_i), \tag{5}$$

$$\partial_{x_i} \to \quad \partial_{z_i} = \frac{1}{z_i'}\,\partial_{x_i}, \text{ with } z_i' := \partial_{x_i} z_i(x_i). \tag{6}$$

In case we want to allow for waves propagating to the left of the x_i-direction the PML-parameters have to satisfy (cf. [13])

$$\begin{array}{ll} a_i(x_i) = b_i(x_i) = 0 & \text{for } x_i \text{ corr. to } \mathbf{x} \in \Omega_O, \\ a_i(x_i) \le 0,\ b_i(x_i) \le 0 & \text{for } x_i \text{ corr. to } \mathbf{x} \in \Omega_{PML}. \end{array}$$

This choice maintains the original equations in the interior domain and implies the solution to be evanescent within the absorbing layer. Moreover, we assume the parameters to be continuous across the interior PML interface $\Omega_{\text{PML}} \cap \Omega_O$ in order to avoid reflections at the interface.

Applying the coordinate transformation mentioned above to the piezoelectric equations (1)-(4) can be interpreted in two ways:

1) as piezoelectric equations with original material parameters stated in complex-valued cartesian coordinates z_i (and derivates with respect to z_i) [10], or,
2) as piezoelectric equations (1)-(2) with material laws

$$\mathbb{T}_{ij} = \tilde{d}_{ijkl}\,\frac{\partial u_k}{\partial x_l} - \tilde{\epsilon}_{kij}\mathbf{E}_k \tag{7}$$

$$\mathbf{D}_i = \tilde{\epsilon}_{ikl}\,\frac{\partial u_l}{\partial x_k} + \tilde{\varepsilon}_{ik}\,\mathbf{E}_k, \tag{8}$$

in the original cartesian coordinates x_i (and derivates with respect to x_i) and modified complex-valued material parameters

$$\tilde{d}_{ijkl} := \frac{z'}{z_j' z_l'}\,c_{ijkl}, \qquad \tilde{\epsilon}_{ijk} := \frac{z'}{z_i' z_k'}\,e_{ijk}, \tag{9}$$

$$\tilde{\varepsilon}_{ij} := \frac{z'}{z_i' z_j'}\,\varepsilon_{ij}, \qquad \tilde{\rho} := z'\rho, \tag{10}$$

with $z' := \Pi_i\, z_i'$. We have to state the material laws in terms of gradients, since the applied transformation does not conserve strains. Note, that the complex-valued tensors $\tilde{d}_{ijkl}$ and $\tilde{\epsilon}_{ijk}$ have minor symmetry properties than the original tensors c_{ijkl} and e_{ijk}.

We gain the complex-valued material parameters of the second approach by applying the technique, presented in [13] for linear elasticity and Maxwell's equations, to the piezoelectric equations. We point out that the material parameters in Ω_O are the original ones, i.e. the physically correct ones.

Here, we realize one further main advantage of PML, namely its implementational simplicity by using the method of coordinate-stretching. We have to extend the implementation either by complex-valued material parameters or by complex-valued coordinates. In Netgen/NGSolve perfectly matched layers are realized by the first approach.

The FE-discretized equations for piezoelectric problems with PML lead to a *complex-symmetric* saddle point problem of the form [11]

$$\left(\begin{bmatrix} K_{uu} & K_{u\Phi} \\ K_{\Phi u} & -K_{\Phi\Phi} \end{bmatrix} - \omega^2 \begin{bmatrix} M_{uu} & 0 \\ 0 & 0 \end{bmatrix} \right) \begin{bmatrix} u_h \\ \Phi_h \end{bmatrix} = \begin{bmatrix} F \\ Q \end{bmatrix}$$

The structure of the piezoelectric system matrices remains unchanged by introducing PML. The change lies only in the complex-symmetry of the system.

C. Application to periodic piezoelectric structures

In the sequel, we assume the underlying structure to be periodic in x_1-direction. We point out that the artifically introduced PML has to obey the same periodicity (cf. Figure 1 (left)). Due to the Floquet-Bloch theorem ([14]) we assume quasi-periodic solutions, i.e.

$$\mathbf{u}(x_1 + p, x_2) = e^{(\alpha + i\beta)p}\mathbf{u}(x_1, x_2), \tag{11}$$

$$\Phi(x_1 + p, x_2) = e^{(\alpha + i\beta)p}\Phi(x_1, x_2). \tag{12}$$

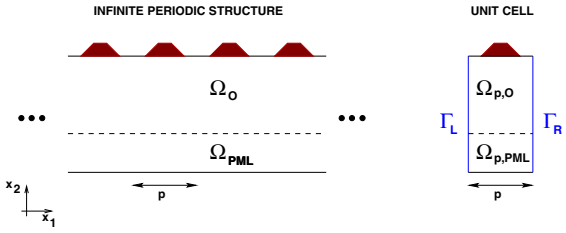

Fig. 1. Periodic structure with PML region and corresponding unit cell

Stating quasi-periodic boundary conditions on the left and right periodic boundary, namely Γ_L and Γ_R (as depictured in figure 1 (right)), we can limit the computational domain to one single unit cell. Since the introduction of the PML-region has not changed the structure of the piezoelectric problem (apart from complex-symmetric matrices), we can directly apply the techniques for periodic problems as developed in [15].

We utilize the Lagrange-parameter formulation [16] in combination with PML. By this, we obtain the discretized system (with $\tilde{u} = (u_h, \Phi_h)^t$)

$$\begin{bmatrix} K - \omega^2 M & (\mathrm{Id}_L - \gamma \mathrm{Id}_R)^t \\ \mathrm{Id}_R - \gamma \mathrm{Id}_L & 0 \end{bmatrix} \begin{bmatrix} \tilde{u} \\ \lambda \end{bmatrix} = \begin{bmatrix} \tilde{F} \\ 0 \end{bmatrix} \qquad (13)$$

involving two parameters - the frequency ω and the periodic propagation parameter $\gamma := e^{(\alpha+i\beta)p}$. We remark that we assume matching meshes (in the sense of periodic meshes) in order to realize the left and right periodic trace operators by the identity matrices $\mathrm{Id}_L, \mathrm{Id}_R$.

Our final goal is to use the PML method for modeling the absorption in the simulation of dispersion relations and the harmonic admittance of periodic structures [15]. Since the main structure of the problem has not altered, we can directly apply the developed techniques.

III. Results and Discussions

In order to evaluate the PML method and to compare it with ABC and FEM/BEM we consider a periodic system of aluminum electrodes on 42° YX-$LiTaO_3$. We choose a 1st-order ABC with total absorption for incidence normal to the the x_1-axis. We will study the harmonic admittance for $\gamma = -1$ (cf. Eq. 13) [1], i.e. the case of an infinitely extended synchronous resonator. For the relative metalization height of 7% employed, mainly a leaky surface acoustic wave (LSAW), predominantly consisting of a horizontally polarized fast shear wave (FSW), exists. Besides the FSW the LSAW contains also a slow shear wave (SSW) contribution. While the FSW part is bounded to the surface, the SSW is radiated to the substrate. Since the LSAW slowness is close to the FSW bulk wave slowness, at about 7% above the resonance frequency, at the so called onset frequency, also the FSW is radiated into the substrate. This is reflected by the conductance of the harmonic admittance (Fig. 5). Since dissipative losses are neglected, the finite quality of the resonance peak (1800 MHz) is due to SSW radiation, while the broad band loss above onset frequency (1920 MHz) is associated with FSW radiation.

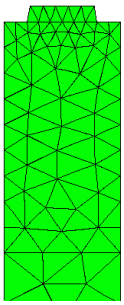

Fig. 2. Mesh for $s = \lambda$. Shown is the upper part of the mesh. The straight line at the bottom is the Ω_O/Ω_{PML} interface.

In the examples the period length is $p = 1.1\mu m$, the thickness, i.e. extent in x_2-direction, of the piezoelectric domain Ω_O is denoted as s, the thickness of the PML layer Ω_{PML} amounts in all cases to 6λ, where $\lambda = 2p$ is the wave length at resonance.

In all computations a mesh of a quality equivalent to that in Fig. 2 (for the case $s = 1\lambda$) and FEM basis functions of third degree are used. The electrode is discretized somewhat finer in order to achieve an accurate approximation of the charge distribution there.

Within the PML layer, Ω_{PML}, the complex coordinate stretching is applied to the x_2-coordinate (Fig. 1). The PML-parameters were chosen as $a_1(x_1) = b_1(x_1) = 0$, $a_2(x_2) = 0$ and $b_2(x_2) = \alpha_{PML}(x_2 - x_{2,PML})$, where $x_{2,PML}$ is the x_2-coordinate of the Ω_O/Ω_{PML} interface.

The PML-parameter α_{PML} governs the attenuation within the absorbing layer. On the one hand, we have to choose the parameter big enough in order to minimize reflections at the outer PML-boundary. On the other hand, the fast varying field near the PML/piezo interface has to be resolved by the chosen FE-discretization in order to avoid spurious reflections at the interface.

The adjustment of α_{PML} is illustrated by the displacement component u_3 at f=1900 MHz (Fig. 3), i.e. below the onset frequency, where only the SSW is radiated. For $\alpha_{PML} = 0.1$ the radiated SSW is reflected at the bottom of the PML layer, which causes a standing wave pattern above the PML/Piezo interface. For $\alpha_{PML} = 0.5$ the absolute value of the radiated wave is constant, as is characteristic for a propagating plane wave. No reflection at the bottom nor at the interface of the PML layer occurs. For $\alpha_{PML} = 10.0$ the SSW is reflected at the interface, since the decay in the PML layer is too steep to be resolved by the chosen FE-discretization. For the further presented numerical tests we agree on $\alpha_{PML} = 0.5$.

The admittances obtained with $\alpha_{PML} = 0.5$ are very close to the results of FEM/BEM computations (Figs. 4,5). The first order ABC, in contrast, does not describe the conductance accurately. The susceptance on the other hand is described accurately for frequencies below the onset frequency. Above, artefacts are due to artificial reflections at the lower bound, since the absorption in normal direction is not suitable for

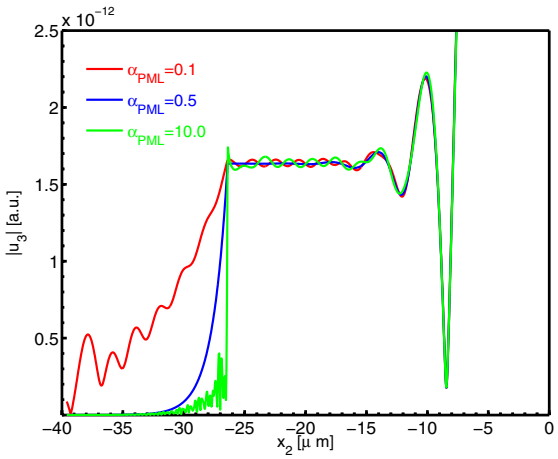

Fig. 3. Dependence of $|u_3|$ on x_2-coordinate, for $x_1 = \frac{p}{2}$ evaluated at f=1900 MHz. The thickness of the piezoelectric domain is $s = 12\lambda$.

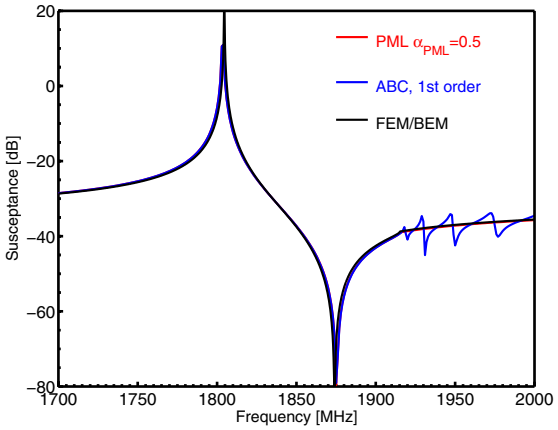

Fig. 4. Susceptance of harmonic admittance for $\gamma = -1$ of Al/42°YX-$LiTaO_3$. Compared are ABC (s=6 λ, blue line), PML (s=6 λ, $\alpha_{PML} = 0.5$, red line) and FEM/BEM methods.

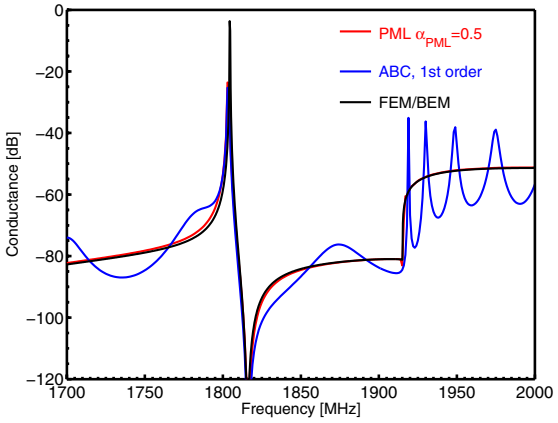

Fig. 5. Conductance of harmonic admittance for $\gamma = -1$ of Al/42°YX-$LiTaO_3$. Compared are ABC (s=6 λ, blue line), PML ($s = 6\lambda$, $\alpha_{PML} = 0.5$, red line) and FEM/BEM methods.

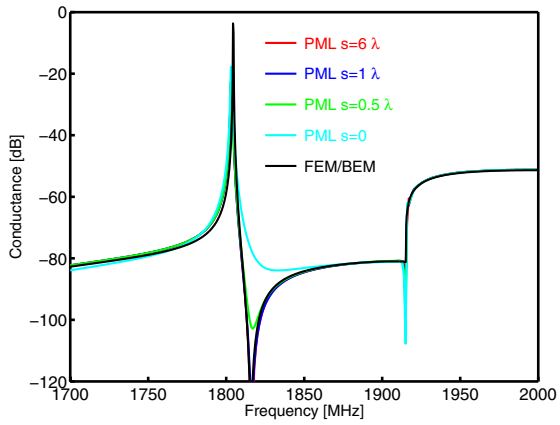

Fig. 6. Conductance of harmonic admittance for $\gamma = -1$ of Al/42°YX-$LiTaO_3$. Compared are results for different depths, s, of the piezoelectric domain with FEM/BEM results.

higher frequencies.

Now the effect of reducing the thickness of the piezoelectric domain, while keeping the discretization fixed, is investigated. Fig. 6 shows the conductances for $s = 0, 0.5, 1.0, 6\lambda$. In the case $s = 0$ the piezoelectric domain is completely absent and the PML layer is directly attached to the electrode. The results are astonishingly stable with respect to variation of s, even for $s = 0$ the essential features of the conductance are preserved, while the susceptance (not shown) is in all cases very close to the FEM/BEM susceptance (cf. Fig. 4).

These findings indicate that within the chosen discretization (see Fig. 2) propagating as well as bounded (decaying) waves are described sufficiently accurate with PML, even for small or vanishing thickness, s, of the piezoelectric domain Ω_{PML}. We demonstrate this now by consideration of the wave fields.

Fig. 3 shows that the wave function has the characteristic of a radiated wave below $x_2 = -15\mu m$ (about 7 λ). At lower depths the bounded parts of the wave function dominate. For f=1900 MHz the u_3-component is mainly bounded. Fig. 7 shows u_3 for varying s. Comparing the wave fields for $s = 0.25, 0.5, 1.0\lambda$ with the wave field of the reference case $s = 12\lambda$, which can be considered as exact solution, it becomes apparent that the fields in the piezoelectric domain (outside the PML) remain unchanged and equal to the fields in the reference case.

The high quality of the description of bulk acoustic wave radiation can be seen by a Fourier transformation of the wave fields below the onset frequency at f=1900 MHz and above the onset frequency at f=1950 MHz (Fig. 8). To this end the wave fields at $x_1 = \frac{p}{2}$ in case of the large piezoelectric domain of thickness $s = 12\lambda$ were Fourier transformed in x_2-direction. Below the onset frequency only the mainly u_2-polarized SSW is radiated, which is reflected in a peak around $k_2 = \frac{\pi}{2p}$. The horizontally polarized FSW is still bounded as the broad peak of u_3 around $k_2 = 0$ reveals. Above the onset frequency the dominating radiation is the FSW radiation which shows up in the peaks around $k_2 = \frac{\pi}{4p}$ in both u_3 and u_2. The SSW radiation at $k_2 = \frac{\pi}{2p}$, however, is also present and its strength

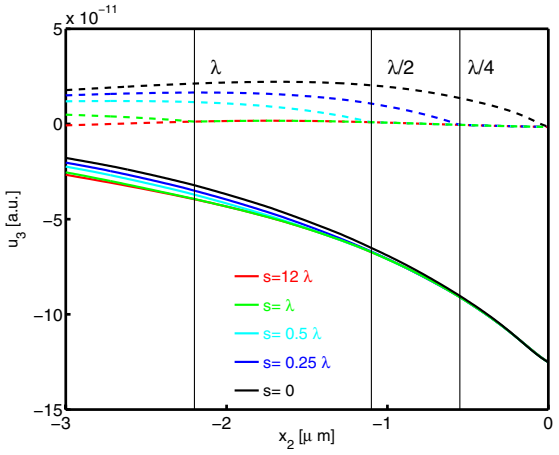

Fig. 7. Real (solid lines) and imaginary (dashed lines) parts of displacement u_3 as function of x_2, for $x_1 = \frac{p}{2}$, evaluated at $f = 1900\ MHz$. The profiles are displayed for different thicknesses (s) of the piezoelectric domain.

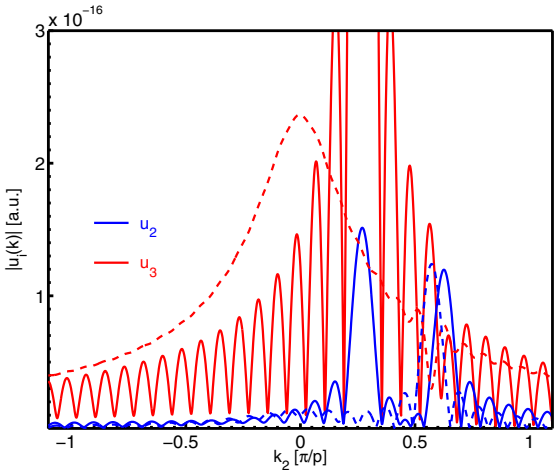

Fig. 8. Fourier transformations in x_2-direction of wave fields u_3 (red line) and u_2 (blue line) for frequencies f=1900 MHz (dashed lines) and f=1950 MHz (solid lines). Only fields in the piezoelectric domain of thickness $s = 12\lambda$ were transformed.

is undiminished with respect to f=1900 MHz. Fig. 8 clearly shows that radiation is only present in negative x_2-direction, i.e. no spurious reflections from the PML/Piezo interface are present.

IV. Conclusions

The infinitely extended piezoelectric halfspace of the substrate of a piezoelectric device was described by a PML layer. The FE-discretized equations of the quasi-periodic FEM problem including PML were derived. For the example of the Al/42°YX-$LiTaO_3$ system results equivalent to FEM/BEM were obtained. By visualizations of the wave fields it was shown that PML provides an excellent description of bulk wave radiation.

References

[1] Y. Zhang, J. Desbois, and L. Boyer, "Characteristic parameters of surface acoustic waves in a periodic metal grating on a piezoelectric substrate," *IEEE Trans. UFFC*, vol. 40, pp. 183–192, May 1993.

[2] P. Ventura, J. M. Hodé, M. Solal, J. Desbois, and J. Ribbe, "Numerical methods for SAW propagation characterization," *IEEE Ultrason. Symp.*, pp. 175–186, 1999.

[3] J. Koskela, V. Plessky, and M.M.Salomaa, "SAW/LSAW COM parameter extraction from computer experiments with harmonic admittance of a periodic array of electrodes," *IEEE Trans. UFFC*, vol. 46, pp. 806–816, 4 1999.

[4] A. Reichinger and A. Baghai-Wadji, "Dynamic 2D-analysis of saw-devices including mass loading," *IEEE Ultrason. Symp.*, pp. 7–10, 1992.

[5] N. Finger, G. Kovacs, J. Schöberl, and U. Langer, "Accurate FEM/BEM-simulation of surface acoustic wave filters," *IEEE Ultrason. Symp.*, pp. 1680–1685, 2003.

[6] B. Engquist and A. Majda, "Absorbing boundary conditions for the numerical simulation of waves," *Mathematics of Computation*, vol. 31, pp. 629–651, 1977.

[7] R. L. Higdon, "Radiation boundary conditions for elastic wave propagation," *SIAM Journal of Numerical Analysis*, vol. 27, pp. 831–870, 1990.

[8] J. P. Berenger, "A perfectly matched layer for the absorption of electromagnetic waves," *Journal of Comp. Phys.*, vol. 114, pp. 185–200, 1994.

[9] W. C. Chew and W. H. Weedon, "A 3D perfectly matched medium from modified maxwell's equations with stretched coordinates," *Microwave and Optical Technology Letters*, vol. 7, pp. 599–604, September 1994.

[10] W. Chew, J. Jin, and E. Michielssen, "Complex coordinate stretching as a generalized absorbing boundary condition," *Micro. Opt. Tech. Lett.*, vol. 15, no. 6, pp. 363–369, 1997.

[11] M. Hofer, N. Finger, G. Kovacs, J. Schöberl, U. Langer, and R. Lerch, "Finite element simulation of bulk- and surface acoustic wave interaction in saw devices," *IEEE Ultrason. Symp.*, pp. 53–56, 2002.

[12] B. Auld, *Acoustic Fields and Waves in Solids*, 2nd ed. Malabar, Florida: Krieger Publishing Company, 1990.

[13] C. Michler, L. Demkowicz, J. Kurtz, and D. Pardo, "Improving the performance of perfectly matched layers by means of hp-adaptivity," *Numerical Methods for Partial Differential Equations*, vol. 23, no. 4, pp. 832–858, 2007.

[14] P. Kuchment, *Floquet Theory For Partial Differential Equations*. Basel: Birkhuser Verlag, 1993.

[15] M. Hofer, N. Finger, J. Schöberl, S. Zaglmayr, U. Langer, and R. Lerch, "Finite element simulation of wave propagation in periodic piezoelectric SAW structures," *IEEE Trans. on UFFC*, vol. 53, no. 6, pp. 1192–1201, 2006.

[16] O. Zienkiewicz and R. Taylor, *The finite element method*. London: McGraw-Hill, 1994.